

# Suppressed $\pi^0$ Production at Large Transverse Momentum in Central Au+Au Collisions at $\sqrt{s_{NN}} = 200$ GeV

S.S. Adler,<sup>5</sup> S. Afanasiev,<sup>17</sup> C. Aidala,<sup>5</sup> N.N. Ajitanand,<sup>43</sup> Y. Akiba,<sup>20,28</sup> J. Alexander,<sup>43</sup> R. Amirikas,<sup>12</sup> L. Aphecetche,<sup>45</sup> S.H. Aronson,<sup>5</sup> R. Auerbeck,<sup>44</sup> T.C. Awes,<sup>35</sup> R. Azmoun,<sup>44</sup> V. Babintsev,<sup>15</sup> A. Baldissieri,<sup>10</sup> K.N. Barish,<sup>6</sup> P.D. Barnes,<sup>27</sup> B. Bassalleck,<sup>33</sup> S. Bathe,<sup>30</sup> S. Batsouli,<sup>9</sup> V. Baublis,<sup>37</sup> A. Bazilevsky,<sup>39,15</sup> S. Belikov,<sup>16,15</sup> Y. Berdnikov,<sup>40</sup> S. Bhagavatula,<sup>16</sup> J.G. Boissevain,<sup>27</sup> H. Borel,<sup>10</sup> S. Borenstein,<sup>25</sup> M.L. Brooks,<sup>27</sup> D.S. Brown,<sup>34</sup> N. Bruner,<sup>33</sup> D. Bucher,<sup>30</sup> H. Buesching,<sup>30</sup> V. Bumazhnov,<sup>15</sup> G. Bunce,<sup>5,39</sup> J.M. Burward-Hoy,<sup>26,44</sup> S. Butsyk,<sup>44</sup> X. Camard,<sup>45</sup> J.-S. Chai,<sup>18</sup> P. Chand,<sup>4</sup> W.C. Chang,<sup>2</sup> S. Chernichenko,<sup>15</sup> C.Y. Chi,<sup>9</sup> J. Chiba,<sup>20</sup> M. Chiu,<sup>9</sup> I.J. Choi,<sup>52</sup> J. Choi,<sup>19</sup> R.K. Choudhury,<sup>4</sup> T. Chujo,<sup>5</sup> V. Cianciolo,<sup>35</sup> Y. Cobigo,<sup>10</sup> B.A. Cole,<sup>9</sup> P. Constantin,<sup>16</sup> D.G. d'Enterria,<sup>45</sup> G. David,<sup>5</sup> H. Delagrange,<sup>45</sup> A. Denisov,<sup>15</sup> A. Deshpande,<sup>39</sup> E.J. Desmond,<sup>5</sup> O. Dietzsch,<sup>41</sup> O. Drapier,<sup>25</sup> A. Drees,<sup>44</sup> K.A. Drees,<sup>5</sup> R. du Rietz,<sup>29</sup> A. Durum,<sup>15</sup> D. Dutta,<sup>4</sup> Y.V. Efremenko,<sup>35</sup> K. El Chenawi,<sup>49</sup> A. Enokizono,<sup>14</sup> H. En'yo,<sup>38,39</sup> S. Esumi,<sup>48</sup> L. Ewell,<sup>5</sup> D.E. Fields,<sup>33,39</sup> F. Fleuret,<sup>25</sup> S.L. Fokin,<sup>23</sup> B.D. Fox,<sup>39</sup> Z. Fraenkel,<sup>51</sup> J.E. Frantz,<sup>9</sup> A. Franz,<sup>5</sup> A.D. Frawley,<sup>12</sup> S.-Y. Fung,<sup>6</sup> S. Garpman,<sup>29,\*</sup> T.K. Ghosh,<sup>49</sup> A. Glenn,<sup>46</sup> G. Gogiberidze,<sup>46</sup> M. Gonin,<sup>25</sup> J. Gosset,<sup>10</sup> Y. Goto,<sup>39</sup> R. Granier de Cassagnac,<sup>25</sup> N. Grau,<sup>16</sup> S.V. Greene,<sup>49</sup> M. Grosse Perdekamp,<sup>39</sup> W. Guryon,<sup>5</sup> H.-Å. Gustafsson,<sup>29</sup> T. Hachiya,<sup>14</sup> J.S. Haggerty,<sup>5</sup> H. Hamagaki,<sup>8</sup> A.G. Hansen,<sup>27</sup> E.P. Hartouni,<sup>26</sup> M. Harvey,<sup>5</sup> R. Hayano,<sup>8</sup> X. He,<sup>13</sup> M. Heffner,<sup>26</sup> T.K. Hemmick,<sup>44</sup> J.M. Heuser,<sup>44</sup> M. Hibino,<sup>50</sup> J.C. Hill,<sup>16</sup> W. Holzmann,<sup>43</sup> K. Homma,<sup>14</sup> B. Hong,<sup>22</sup> A. Hoover,<sup>34</sup> T. Ichihara,<sup>38,39</sup> V.V. Ikonnikov,<sup>23</sup> K. Imai,<sup>24,38</sup> L.D. Isenhower,<sup>1</sup> M. Ishihara,<sup>38</sup> M. Issah,<sup>43</sup> A. Isupov,<sup>17</sup> B.V. Jacak,<sup>44</sup> W.Y. Jang,<sup>22</sup> Y. Jeong,<sup>19</sup> J. Jia,<sup>44</sup> O. Jinnouchi,<sup>38</sup> B.M. Johnson,<sup>5</sup> S.C. Johnson,<sup>26</sup> K.S. Joo,<sup>31</sup> D. Jouan,<sup>36</sup> S. Kametani,<sup>8,50</sup> N. Kamihara,<sup>47,38</sup> J.H. Kang,<sup>52</sup> S.S. Kapoor,<sup>4</sup> K. Katou,<sup>50</sup> S. Kelly,<sup>9</sup> B. Khachaturov,<sup>51</sup> A. Khanzadeev,<sup>37</sup> J. Kikuchi,<sup>50</sup> D.H. Kim,<sup>31</sup> D.J. Kim,<sup>52</sup> D.W. Kim,<sup>19</sup> E. Kim,<sup>42</sup> G.-B. Kim,<sup>25</sup> H.J. Kim,<sup>52</sup> E. Kistenev,<sup>5</sup> A. Kiyomichi,<sup>48</sup> K. Kiyoyama,<sup>32</sup> C. Klein-Boesing,<sup>30</sup> H. Kobayashi,<sup>38,39</sup> L. Kochenda,<sup>37</sup> V. Kochetkov,<sup>15</sup> D. Koehler,<sup>33</sup> T. Kohama,<sup>14</sup> M. Kopytine,<sup>44</sup> D. Kotchetkov,<sup>6</sup> A. Kozlov,<sup>51</sup> P.J. Kroon,<sup>5</sup> C.H. Kuberg,<sup>1,27</sup> K. Kurita,<sup>39</sup> Y. Kuroki,<sup>48</sup> M.J. Kweon,<sup>22</sup> Y. Kwon,<sup>52</sup> G.S. Kyle,<sup>34</sup> R. Lacey,<sup>43</sup> V. Ladygin,<sup>17</sup> J.G. Lajoie,<sup>16</sup> A. Lebedev,<sup>16,23</sup> S. Leckey,<sup>44</sup> D.M. Lee,<sup>27</sup> S. Lee,<sup>19</sup> M.J. Leitch,<sup>27</sup> X.H. Li,<sup>6</sup> H. Lim,<sup>42</sup> A. Litvinenko,<sup>17</sup> M.X. Liu,<sup>27</sup> Y. Liu,<sup>36</sup> C.F. Maguire,<sup>49</sup> Y.I. Makdisi,<sup>5</sup> A. Malakhov,<sup>17</sup> V.I. Manko,<sup>23</sup> Y. Mao,<sup>7,38</sup> G. Martinez,<sup>45</sup> M.D. Marx,<sup>44</sup> H. Masui,<sup>48</sup> F. Matathias,<sup>44</sup> T. Matsumoto,<sup>8,50</sup> P.L. McGaughey,<sup>27</sup> E. Melnikov,<sup>15</sup> F. Messer,<sup>44</sup> Y. Miake,<sup>48</sup> J. Milan,<sup>43</sup> T.E. Miller,<sup>49</sup> A. Milov,<sup>44,51</sup> S. Mioduszewski,<sup>5</sup> R.E. Mischke,<sup>27</sup> G.C. Mishra,<sup>13</sup> J.T. Mitchell,<sup>5</sup> A.K. Mohanty,<sup>4</sup> D.P. Morrison,<sup>5</sup> J.M. Moss,<sup>27</sup> F. Mühlbacher,<sup>44</sup> D. Mukhopadhyay,<sup>51</sup> M. Muniruzzaman,<sup>6</sup> J. Murata,<sup>38,39</sup> S. Nagamiya,<sup>20</sup> J.L. Nagle,<sup>9</sup> T. Nakamura,<sup>14</sup> B.K. Nandi,<sup>6</sup> M. Nara,<sup>48</sup> J. Newby,<sup>46</sup> P. Nilsson,<sup>29</sup> A.S. Nyanin,<sup>23</sup> J. Nystrand,<sup>29</sup> E. O'Brien,<sup>5</sup> C.A. Ogilvie,<sup>16</sup> H. Ohnishi,<sup>5,38</sup> I.D. Ojha,<sup>49,3</sup> K. Okada,<sup>38</sup> M. Ono,<sup>48</sup> V. Onuchin,<sup>15</sup> A. Oskarsson,<sup>29</sup> I. Otterlund,<sup>29</sup> K. Oyama,<sup>8</sup> K. Ozawa,<sup>8</sup> D. Pal,<sup>51</sup> A.P.T. Palounek,<sup>27</sup> V.S. Pantuev,<sup>44</sup> V. Papavassiliou,<sup>34</sup> J. Park,<sup>42</sup> A. Parmar,<sup>33</sup> S.F. Pate,<sup>34</sup> T. Peitzmann,<sup>30</sup> J.-C. Peng,<sup>27</sup> V. Peresedov,<sup>17</sup> C. Pinkenburg,<sup>5</sup> R.P. Pisani,<sup>5</sup> F. Plasil,<sup>35</sup> M.L. Purschke,<sup>5</sup> A. Purwar,<sup>44</sup> J. Rak,<sup>16</sup> I. Ravinovich,<sup>51</sup> K.F. Read,<sup>35,46</sup> M. Reuter,<sup>44</sup> K. Reygers,<sup>30</sup> V. Riabov,<sup>37,40</sup> Y. Riabov,<sup>37</sup> G. Roche,<sup>28</sup> A. Romana,<sup>25</sup> M. Rosati,<sup>16</sup> P. Rosnet,<sup>28</sup> S.S. Ryu,<sup>52</sup> M.E. Sadler,<sup>1</sup> N. Saito,<sup>38,39</sup> T. Sakaguchi,<sup>8,50</sup> M. Sakai,<sup>32</sup> S. Sakai,<sup>48</sup> V. Samsonov,<sup>37</sup> L. Sanfratello,<sup>33</sup> R. Santo,<sup>30</sup> H.D. Sato,<sup>24,38</sup> S. Sato,<sup>5,48</sup> S. Sawada,<sup>20</sup> Y. Schutz,<sup>45</sup> V. Semenov,<sup>15</sup> R. Seto,<sup>6</sup> M.R. Shaw,<sup>1,27</sup> T.K. Shea,<sup>5</sup> T.-A. Shibata,<sup>47,38</sup> K. Shigaki,<sup>14,20</sup> T. Shiina,<sup>27</sup> C.L. Silva,<sup>41</sup> D. Silvermyr,<sup>27,29</sup> K.S. Sim,<sup>22</sup> C.P. Singh,<sup>3</sup> V. Singh,<sup>3</sup> M. Sivertz,<sup>5</sup> A. Soldatov,<sup>15</sup> R.A. Soltz,<sup>26</sup> W.E. Sondheim,<sup>27</sup> S.P. Sorensen,<sup>46</sup> I.V. Sourikova,<sup>5</sup> F. Staley,<sup>10</sup> P.W. Stankus,<sup>35</sup> E. Stenlund,<sup>29</sup> M. Stepanov,<sup>34</sup> A. Ster,<sup>21</sup> S.P. Stoll,<sup>5</sup> T. Sugitate,<sup>14</sup> J.P. Sullivan,<sup>27</sup> E.M. Takagui,<sup>41</sup> A. Taketani,<sup>38,39</sup> M. Tamai,<sup>50</sup> K.H. Tanaka,<sup>20</sup> Y. Tanaka,<sup>32</sup> K. Tanida,<sup>38</sup> M.J. Tannenbaum,<sup>5</sup> P. Tarján,<sup>11</sup> J.D. Tepe,<sup>1,27</sup> T.L. Thomas,<sup>33</sup> J. Tojo,<sup>24,38</sup> H. Torii,<sup>24,38</sup> R.S. Towell,<sup>1</sup> I. Tserruya,<sup>51</sup> H. Tsuruoka,<sup>48</sup> S.K. Tuli,<sup>3</sup> H. Tydesjö,<sup>29</sup> N. Tyurin,<sup>15</sup> H.W. van Hecke,<sup>27</sup> J. Velkovska,<sup>5,44</sup> M. Velkovsky,<sup>44</sup> L. Villatte,<sup>46</sup> A.A. Vinogradov,<sup>23</sup> M.A. Volkov,<sup>23</sup> E. Vznuzdaev,<sup>37</sup> X.R. Wang,<sup>13</sup> Y. Watanabe,<sup>38,39</sup> S.N. White,<sup>5</sup> F.K. Wohn,<sup>16</sup> C.L. Woody,<sup>5</sup> W. Xie,<sup>6</sup> Y. Yang,<sup>7</sup> A. Yanovich,<sup>15</sup> S. Yokkaichi,<sup>38,39</sup> G.R. Young,<sup>35</sup> I.E. Yushmanov,<sup>23</sup> W.A. Zajc,<sup>9,†</sup> C. Zhang,<sup>9</sup> S. Zhou,<sup>7,51</sup> L. Zolin,<sup>17</sup>

(PHENIX Collaboration)

<sup>1</sup> Abilene Christian University, Abilene, TX 79699, USA

<sup>2</sup> Institute of Physics, Academia Sinica, Taipei 11529, Taiwan

<sup>3</sup> Department of Physics, Banaras Hindu University, Varanasi 221005, India

<sup>4</sup> Bhabha Atomic Research Centre, Bombay 400 085, India

<sup>5</sup> Brookhaven National Laboratory, Upton, NY 11973-5000, USA

<sup>6</sup> University of California - Riverside, Riverside, CA 92521, USA

<sup>7</sup> China Institute of Atomic Energy (CIAE), Beijing, People's Republic of China

<sup>8</sup> Center for Nuclear Study, Graduate School of Science, University of Tokyo, 7-3-1 Hongo, Bunkyo, Tokyo 113-0033, Japan

- <sup>9</sup> *Columbia University, New York, NY 10027 and Nevis Laboratories, Irvington, NY 10533, USA*
- <sup>10</sup> *Dapnia, CEA Saclay, Bat. 703, F-91191, Gif-sur-Yvette, France*
- <sup>11</sup> *Debrecen University, H-4010 Debrecen, Egyetem tér 1, Hungary*
- <sup>12</sup> *Florida State University, Tallahassee, FL 32306, USA*
- <sup>13</sup> *Georgia State University, Atlanta, GA 30303, USA*
- <sup>14</sup> *Hiroshima University, Kagamiyama, Higashi-Hiroshima 739-8526, Japan*
- <sup>15</sup> *Institute for High Energy Physics (IHEP), Protvino, Russia*
- <sup>16</sup> *Iowa State University, Ames, IA 50011, USA*
- <sup>17</sup> *Joint Institute for Nuclear Research, 141980 Dubna, Moscow Region, Russia*
- <sup>18</sup> *KAERI, Cyclotron Application Laboratory, Seoul, South Korea*
- <sup>19</sup> *Kangnung National University, Kangnung 210-702, South Korea*
- <sup>20</sup> *KEK, High Energy Accelerator Research Organization, Tsukuba-shi, Ibaraki-ken 305-0801, Japan*
- <sup>21</sup> *KFKI Research Institute for Particle and Nuclear Physics (RMKI), H-1525 Budapest 114, POBox 49, Hungary*
- <sup>22</sup> *Korea University, Seoul, 136-701, Korea*
- <sup>23</sup> *Russian Research Center “Kurchatov Institute”, Moscow, Russia*
- <sup>24</sup> *Kyoto University, Kyoto 606, Japan*
- <sup>25</sup> *Laboratoire Leprince-Ringuet, Ecole Polytechnique, CNRS-IN2P3, Route de Saclay, F-91128, Palaiseau, France*
- <sup>26</sup> *Lawrence Livermore National Laboratory, Livermore, CA 94550, USA*
- <sup>27</sup> *Los Alamos National Laboratory, Los Alamos, NM 87545, USA*
- <sup>28</sup> *LPC, Université Blaise Pascal, CNRS-IN2P3, Clermont-Fd, 63177 Aubiere Cedex, France*
- <sup>29</sup> *Department of Physics, Lund University, Box 118, SE-221 00 Lund, Sweden*
- <sup>30</sup> *Institut fuer Kernphysik, University of Muenster, D-48149 Muenster, Germany*
- <sup>31</sup> *Myongji University, Yongin, Kyonggido 449-728, Korea*
- <sup>32</sup> *Nagasaki Institute of Applied Science, Nagasaki-shi, Nagasaki 851-0193, Japan*
- <sup>33</sup> *University of New Mexico, Albuquerque, NM, USA*
- <sup>34</sup> *New Mexico State University, Las Cruces, NM 88003, USA*
- <sup>35</sup> *Oak Ridge National Laboratory, Oak Ridge, TN 37831, USA*
- <sup>36</sup> *IPN-Orsay, Universite Paris Sud, CNRS-IN2P3, BP1, F-91406, Orsay, France*
- <sup>37</sup> *PNPI, Petersburg Nuclear Physics Institute, Gatchina, Russia*
- <sup>38</sup> *RIKEN (The Institute of Physical and Chemical Research), Wako, Saitama 351-0198, JAPAN*
- <sup>39</sup> *RIKEN BNL Research Center, Brookhaven National Laboratory, Upton, NY 11973-5000, USA*
- <sup>40</sup> *St. Petersburg State Technical University, St. Petersburg, Russia*
- <sup>41</sup> *Universidade de São Paulo, Instituto de Física, Caixa Postal 66318, São Paulo CEP05315-970, Brazil*
- <sup>42</sup> *System Electronics Laboratory, Seoul National University, Seoul, South Korea*
- <sup>43</sup> *Chemistry Department, Stony Brook University, SUNY, Stony Brook, NY 11794-3400, USA*
- <sup>44</sup> *Department of Physics and Astronomy, Stony Brook University, SUNY, Stony Brook, NY 11794, USA*
- <sup>45</sup> *SUBATECH (Ecole des Mines de Nantes, CNRS-IN2P3, Université de Nantes) BP 20722 - 44307, Nantes, France*
- <sup>46</sup> *University of Tennessee, Knoxville, TN 37996, USA*
- <sup>47</sup> *Department of Physics, Tokyo Institute of Technology, Tokyo, 152-8551, Japan*
- <sup>48</sup> *Institute of Physics, University of Tsukuba, Tsukuba, Ibaraki 305, Japan*
- <sup>49</sup> *Vanderbilt University, Nashville, TN 37235, USA*
- <sup>50</sup> *Waseda University, Advanced Research Institute for Science and Engineering, 17 Kikui-cho, Shinjuku-ku, Tokyo 162-0044, Japan*
- <sup>51</sup> *Weizmann Institute, Rehovot 76100, Israel*
- <sup>52</sup> *Yonsei University, IPAP, Seoul 120-749, Korea*

(October 24, 2018)

Transverse momentum spectra of neutral pions in the range  $1 < p_T < 10$  GeV/ $c$  have been measured at mid-rapidity by the PHENIX experiment at RHIC in Au+Au collisions at  $\sqrt{s_{NN}} = 200$  GeV. The  $\pi^0$  multiplicity in central reactions is significantly below the yields measured at the same  $\sqrt{s_{NN}}$  in peripheral Au+Au and  $p + p$  reactions scaled by the number of nucleon-nucleon collisions. For the most central bin, the suppression factor is  $\sim 2.5$  at  $p_T = 2$  GeV/ $c$  and increases to  $\sim 4-5$  at  $p_T \approx 4$  GeV/ $c$ . At larger  $p_T$ , the suppression remains constant within errors. The deficit is already apparent in semi-peripheral reactions and increases smoothly with centrality.

PACS numbers: 25.75.Dw

High energy collisions of heavy ions provide the means to study Quantum Chromodynamics (QCD) at energy densities where lattice calculations [1] predict a transi-

tion from hadronic matter to a deconfined, chirally symmetric plasma of quarks and gluons (QGP). The large center-of-mass energies,  $\sqrt{s_{NN}} \approx 200$  GeV, available in

Au+Au collisions at the Relativistic Heavy Ion Collider (RHIC), have resulted in a significant production of high transverse momentum hadrons ( $p_T > 2$  GeV/ $c$ ) for the first time in heavy-ion physics. High  $p_T$  particle production in hadronic collisions results from the fragmentation of quarks and gluons emerging from the initial high  $Q^2$  parton-parton scatterings [2]. Thus, hard processes in nucleus-nucleus ( $AA$ ) collisions provide direct information on the early partonic phases of the reaction. In the absence of nuclear medium effects, hard scattering yields in  $AA$  reactions are expected to scale like an incoherent superposition of nucleon-nucleon ( $NN$ ) collisions because of the small probability of hard scattering processes per  $NN$  collision. In  $AA$  reactions, the number of  $NN$  collisions ( $N_{coll}$ ) at impact parameter  $b$  is simply proportional to the geometric nuclear overlap function,  $T_{AA}(b)$ , and can be calculated in an eikonal approach [3]. After scaling by the nuclear geometry, spectra of high  $p_T$  particles measured in  $AA$  reactions can be compared to the baseline “vacuum” ( $p + p$ ,  $p + \bar{p}$ ) and “cold medium” ( $p$ ,  $d + A$ ) data, as well as to perturbative [4–7] and “classical” [8] QCD predictions. Any departure from the expected  $N_{coll}$ -scaled result provides information on the strongly interacting medium in central heavy-ion reactions.

One of the most significant observations from the first RHIC run (Run-1) was the suppressed yield of moderately high  $p_T$  neutral pions ( $p_T \approx 1.5 - 4.0$  GeV/ $c$ ) in central Au+Au at  $\sqrt{s_{NN}} = 130$  GeV with respect to the  $N_{coll}$ -scaled  $p + p$  and peripheral Au+Au data [9]. This result points to strong medium effects present in central Au+Au and has triggered extensive theoretical studies on its origin [4–8,10–13]. Most of these studies are based on the prediction [14,15] that a QGP would induce multiple gluon radiations from the scattered fast partons, effectively leading to a suppression of high  $p_T$  hadronic fragmentation products (“jet quenching”). Alternative interpretations have been proposed based on initial-state gluon saturation [8] or final-state hadronic interactions [13].

This Letter presents  $\pi^0$  results obtained by the PHENIX experiment in Au+Au collisions at  $\sqrt{s_{NN}} = 200$  GeV and compares them to the  $p + p \rightarrow \pi^0 X$  data measured in the same experiment at the same center-of-mass energy [16]. During the 2001-2002 RHIC run (Run-2), PHENIX obtained  $\pi^0$  data measured in the electromagnetic calorimeter (EMCal). The present analysis uses 30 million minimum bias events, triggered by a coincidence between the Zero Degree Calorimeters (ZDC) and the Beam-Beam Counters (BBC), with vertex position  $|z| < 30$  cm. In Run-2, the PHENIX EMCal was fully instrumented providing a total solid angle coverage at mid-rapidity of approximately  $\Delta\eta = 0.7$  and  $\Delta\phi = \pi$  and the total collected  $\pi^0$  statistics was a factor of  $\sim 100$  larger than in Run-1 [9]. The combination of larger acceptance, high statistics, and the measurement of  $p + p$

data in the same detector permits a precise study of the high  $p_T$   $\pi^0$  production mechanisms in  $AA$  collisions at RHIC.

Neutral pions are reconstructed via their  $\pi^0 \rightarrow \gamma\gamma$  decay through an invariant mass analysis of  $\gamma$  pairs detected in the EMCal [17] which consists of 6 lead-scintillator (PbSc) and 2 lead-glass Čerenkov (PbGl) sectors. The large radial distance of the calorimeters to the interaction region ( $> 5$  m) and their fine granularity ( $\Delta\eta \times \Delta\phi \approx 0.01 \times 0.01$ ) keep the tower occupancy low,  $< 10\%$  even in the highest multiplicity Au+Au events. The energy calibration is obtained from beam tests and, in the case of PbSc, from cosmic rays data and the known minimum ionizing energy peak of charged hadrons traversing the calorimeter. It is then confirmed using the  $\pi^0$  mass, as well as the agreement of the calorimeter energy with the measured momentum of identified electrons. The systematic error on the absolute energy scale is less than 1.5%. Photon-like clusters are identified in the EMCal by applying time-of-flight and shower profile cuts [17]. The selected clusters are binned in pair invariant mass  $m_{\gamma\gamma}$  and  $p_T$ . An additional energy asymmetry cut,  $|E_{\gamma 1} - E_{\gamma 2}| / (E_{\gamma 1} + E_{\gamma 2}) < 0.7$  (PbGl), 0.8 (PbSc), is applied to the reconstructed pairs. The signal-to-background in peripheral (central) is approximately 20 (5) and 0.5 (0.01) for the highest and lowest  $p_T$ , respectively. The combinatorial background is estimated and subtracted by mixing clusters from different events with similar centrality and vertex, and normalizing the distribution in a region outside the  $\pi^0$  mass peak. The  $\pi^0$  yield in each  $p_T$  bin is determined by integrating the subtracted  $m_{\gamma\gamma}$  distribution in a  $\pm 3\sigma$  window determined by a  $p_T$ -dependent parameterization of Gaussian fits to the  $\pi^0$  peaks.

The raw PbSc and PbGl  $\pi^0$  spectra are normalized to one unit of rapidity and full azimuth (this acceptance correction rises quickly with  $p_T$  up to a  $\sim 1/0.35$  pure geometric factor). The spectra are further corrected for (i) the detector response (energy resolution, dead areas), (ii) the reconstruction efficiency (analysis cuts), and (iii) the occupancy effects (cluster overlaps). These corrections are quantified by embedding simulated single  $\pi^0$ 's from a full PHENIX GEANT [18] simulation into real events, and analyzing the merged events with the same analysis cuts used to obtain the real yields. Each correction is determined, for each centrality bin, as the ratio of the input (simulated) to the reconstructed  $p_T$  distribution. The overall yield correction amounts to  $\sim 2.5$  with a centrality dependence  $\lesssim 25\%$ . The losses are dominated by fiducial and asymmetry cuts.

The main sources of systematic errors in the PbSc and PbGl measurements are due to the uncertainties in: (i) the yield extraction, (ii) the yield correction, and (iii) the energy scale. The relative contributions of these effects to the total error differ for the PbSc and PbGl (Table I). The weighted average of the two independent measure-

ments reduces the total error. The nominal energy resolution [17] is adjusted in the simulation to reproduce the true width of the  $\pi^0$  peak observed at each  $p_T$ , smearing the energies with a constant term of 7% for PbSc and  $\sim 9\%$  for PbGl. The shape, position, and width of the  $\pi^0$  peak measured in all different centralities are then confirmed to be well reproduced by the embedded data. The final systematic errors on the spectra are at the level of  $\sim 10\%$  at 1 GeV/c and  $\sim 17\%$  at the highest  $p_T$  (Table I). A correction for the true mean value of the  $p_T$  bin is applied to the steeply falling spectra. No corrections have been applied to account for the contribution of feed-down  $\pi^0$ 's (mainly coming from  $K_s^0$  and  $\eta$  decays) which are  $< 5\%$  based on HIJING [19] simulations.

The event centrality is determined by correlating the charge detected in the BBC with the energy measured in the ZDC detectors. A Glauber model Monte Carlo (MC) combined with a simulation of the BBC and ZDC responses [20–22] gives an estimate of the associated number of binary collisions ( $N_{coll}$ ) and participating nucleons ( $N_{part}$ ) in each centrality bin (Table II). The fully corrected and combined PbSc and PbGl  $\pi^0$   $p_T$  distributions are shown in Fig. 1 for minimum bias and for 9 centrality bins scaled by factors of 10 for clarity.

We quantify the medium effects on high  $p_T$  production in AA collisions with the *nuclear modification factor* given by the ratio of the measured AA invariant yields to the  $NN$  collision scaled  $p + p$  invariant yields:

$$R_{AA}(p_T) = \frac{(1/N_{AA}^{evt}) d^2 N_{AA}^{\pi^0} / dp_T dy}{\langle N_{coll} \rangle / \sigma_{pp}^{inel} \times d^2 \sigma_{pp}^{\pi^0} / dp_T dy}, \quad (1)$$

where the  $\langle N_{coll} \rangle / \sigma_{pp}^{inel}$  is just the average Glauber nuclear overlap function,  $\langle T_{AuAu} \rangle$ , in the centrality bin under consideration (Table II).  $R_{AA}(p_T)$  measures the deviation of AA data from an incoherent superposition of  $NN$  collisions. For  $p_T \lesssim 2$  GeV/c,  $R_{AA}$  is known to be below unity, since the bulk of particle production is due to soft processes which scale closer to the number of participant nucleons [20] than to  $N_{coll}$ .

Figure 2 shows  $R_{AA}$  as a function of  $p_T$  for  $\pi^0$  measured in 0-10% central (closed circles) and 80-92% peripheral (open circles) Au+Au. The PHENIX  $p + p \rightarrow \pi^0$  data [16] is used as the reference in the denominator. The  $R_{AA}$  values for central collisions are noticeably below unity, as found at 130 GeV [9], and in contrast to the enhanced high  $p_T$   $\pi^0$  production ( $R_{AA} > 1$ ) observed at CERN-SPS energies [23] and interpreted in terms of initial-state  $p_T$  broadening effects (“Cronin effect” [24]). Within errors, peripheral Au+Au collisions behave like a superposition of  $p + p$  collisions with regard to high  $p_T$   $\pi^0$  production ( $R_{AA} \approx 1$ ). In central collisions, the suppression is smallest at 2 GeV/c and increases to an approximately constant suppression factor of  $1/R_{AA} \approx 4-5$  over the  $p_T$  range of 4 - 10 GeV/c,  $\sim 30\%$  above the expectation from  $N_{part}$  scaling (dotted line in Fig. 2).

The magnitude and  $p_T$  dependence of  $R_{AA}$  (corresponding to parton fractional momenta  $x \approx 2p_T/\sqrt{s} \sim 0.02 - 0.1$  at midrapidity), is inconsistent with the expectations of leading-twist “shadowing” effects on the nuclear parton distribution functions alone [25]. Different jet quenching calculations [4–7,10–12], based on medium-induced radiative energy loss, can reproduce the magnitude of the  $\pi^0$  suppression assuming the formation of a hot and dense partonic system. The predicted  $p_T$  dependence of the quenching, however, varies in the different models. All models that include the Landau-Pomeranchuk-Migdal (LPM) interference effect [15,26] predict  $R_{AA}$  effectively  $\propto \sqrt{p_T}$  [10]. Such a trend is not compatible with our data over the entire  $p_T$  range. Analyses which combine LPM jet quenching together with shadowing and initial-state  $p_T$  broadening generally reproduce the whole  $p_T$  dependence of the  $\pi^0$  suppression [4], as do recent approaches that take into account detailed balance between parton emission and absorption [7]. However, based solely on the data presented here, we are not able to distinguish between partonic or hadronic [13] energy loss scenarios.

The centrality dependence of the high  $p_T$   $\pi^0$  suppression is shown in Fig. 3 as a function of  $N_{part}$ . The suppression is characterized as the ratio of Au+Au over  $p + p$  yields integrated above 4 GeV/c and normalized using two different scalings.  $R_{AA}$  (circles) denotes the  $N_{coll}$  scaling as in Eq. (1), whereas  $R_{AA}^{part}$  (crosses) indicates  $N_{part}$  scaling expected in scenarios dominated either by gluon saturation [8] or by surface emission of the quenched jets [10]. Fig. 3 indicates that the transition from the  $N_{coll}$  scaling behaviour ( $R_{AA} \sim 1$ ) apparent in the most peripheral region, to the strong suppression seen in central reactions ( $R_{AA} \sim 0.25$ ) is smooth. In addition, although there is no exact participant scaling ( $R_{AA}^{part} > 1$  for all centralities), the  $\pi^0$  production per participant pair above 4 GeV/c is approximately constant over a wide range of intermediate centralities, in qualitative agreement with a parton saturation model prediction [8].

In summary, transverse momentum spectra of neutral pions have been measured at mid-rapidity up to  $p_T \approx 10$  GeV/c for 9 centrality bins of Au+Au collisions at  $\sqrt{s_{NN}} = 200$  GeV. The spectral shape and invariant yield for peripheral reactions are consistent with those of  $p + p$  reactions scaled by the average number of inelastic  $NN$  collisions. Central yields, on the other hand, are significantly lower than peripheral Au+Au and  $p + p$  scaled yields, as found at  $\sqrt{s_{NN}} = 130$  GeV. The observed suppression increases slowly with  $p_T$  to as much as a factor 4-5 in the 10% most central collisions, remaining constant within errors above  $\sim 4$  GeV/c. The suppression is already apparent in semi-peripheral reactions and increases smoothly with centrality. The magnitude of the deficit can be reproduced by parton energy loss calculations in an opaque medium, but its  $p_T$  and centrality dependence puts strong constraints on the details of en-

ergy loss and the properties of the medium. The role of initial-state effects, including shadowing,  $p_T$  broadening, and gluon saturation will be studied with data from the recent RHIC run using d+Au, where final-state medium effects such as jet quenching are absent.

We thank the staff of the Collider-Accelerator and Physics Departments at BNL for their vital contributions. We acknowledge support from the Department of Energy and NSF (U.S.A.), MEXT and JSPS (Japan), CNPq and FAPESP (Brazil), NSFC (China), CNRS-IN2P3 and CEA (France), BMBF, DAAD, and AvH (Germany), OTKA (Hungary), DAE and DST (India), ISF (Israel), KRF and CHEP (Korea), RAS, RMAE, and RMS (Russia), VR and KAW (Sweden), U.S. CRDF for the FSU, US-Hungarian NSF-OTKA-MTA, and US-Israel BSF.

\* Deceased

† Spokesperson: zajc@nevis.columbia.edu

- [1] See E. Laermann and O. Philipsen, hep-ph/0303042 (to appear in Ann. Rev. Nuc. Part. Sci.), for a recent review.
- [2] J.F. Owens *et al.*, Phys. Rev. **D18**, 1501 (1978).
- [3] R.J. Glauber and G. Matthiae, Nucl. Phys. B **21**, 135 (1970).
- [4] I. Vitev and M. Gyulassy, Phys. Rev. Lett. **89** (2002) 252301.
- [5] S. Jeon, J. Jalilian-Marian and I. Sarcevic (to appear in Phys. Lett. **B**), nucl-th/0208012.
- [6] G.G. Barnafoldi, P. Levai, G. Papp, G. Fai, and Y. Zhang, nucl-th/0212111.
- [7] X. N. Wang, Nucl. Phys. **A715**, 775 (2003).
- [8] D. Kharzeev, E. Levin and L. McLerran (to appear in Phys. Lett. **B**), hep-ph/0210332.
- [9] K. Adcox *et al.* [PHENIX Collaboration], Phys. Rev. Lett. **88**, 022301 (2002).
- [10] B. Müller, arXiv:nucl-th/0208038, and references therein.
- [11] F. Arleo, J. High Energy Phys. **11**, 44 (2002).
- [12] C. A. Salgado and U. A. Wiedemann, hep-ph/0302184.
- [13] K. Gallmeister, C. Greiner and Z. Xu (to appear in Phys. Rev. **C**), hep-ph/0212295.
- [14] M. Gyulassy and M. Plümer, Phys. Lett. **B243**, 432 (1990); X.N. Wang and M. Gyulassy, Phys. Rev. Lett. **68**, 1480 (1992).
- [15] R. Baier, D. Schiff and B.G. Zakharov, Annu. Rev. Nucl. Part. Sci. **50**, 37 (2000), and references therein.
- [16] S.S. Adler *et al.* [PHENIX Collaboration], submitted to Phys. Rev. Lett.
- [17] L. Aphecetche *et al.* [PHENIX Collaboration], Nucl. Instrum. Methods **A499**, 521 (2003).
- [18] GEANT 3.21, CERN program library.
- [19] X. N. Wang and M. Gyulassy, Phys. Rev. **D44**, 3501 (1991).
- [20] K. Adcox *et al.* [PHENIX Collaboration], Phys. Rev. Lett. **86**, 3500 (2001).

- [21] The Run-2 minimum bias trigger is inefficient for very peripheral reactions and records  $92.2^{+2.5}_{-3.0}$ % of  $\sigma_{AuAu}$ .
- [22] Woods-Saxon Au nuclear radius  $R = 6.38^{+0.27}_{-0.13}$  fm, diffusivity  $a = 0.53 \pm 0.01$  fm [B. Hahn, D.G. Ravenhall and R. Hofstadter, Phys. Rev. **101**, 1131 (1956)], and nucleon-nucleon cross section  $\sigma_{NN}^{inel} = 42 \pm 3$  mb.
- [23] M.M. Aggarwal *et al.* [WA98 Collaboration], Eur. Phys. J. **C23**, 225 (2002).
- [24] D. Antreasyan *et al.*, Phys. Rev. **D19**, 764 (1979).
- [25] K. J. Eskola, V. J. Kolhinen and C. A. Salgado, Eur. Phys. J. **C 9**, 61 (1999); S. R. Klein and R. Vogt, Phys. Rev. **C67**, 047901 (2003).
- [26] M. Gyulassy, P. Levai and I. Vitev, Phys. Rev. Lett. **85**, 5535 (2000), Nucl. Phys. B **594**, 371 (2001).

TABLE I. Summary of the dominant sources of systematic errors on the PbSc and PbGl  $\pi^0$  yields, and total errors on the combined measurements. The error ranges are quoted for the lowest to highest  $p_T$  values. For the combined  $\pi^0$  spectra and  $R_{AA}$ , we quote the approximate i) statistical, ii) point-to-point systematic, and iii) absolute normalization (for most central and peripheral reactions) errors.

Source	syst. error PbSc		syst. error PbGl	
Yield extraction	10%		6 - 7%	
Yield correction	8%		8%	
Energy scale	3 - 11%		7 - 13%	
Total error (%)	stat.	syst.	normalization	
			central	peripheral
Spectra	2 - 40	10 - 17	5	5
$R_{AA}$	2 - 45	11 - 22	14	30

TABLE II. Centrality bin, average nuclear overlap function, number of  $NN$  collisions, and number of participant nucleons obtained from a Glauber MC [21,22] and the BBC and ZDC responses for Au+Au at  $\sqrt{s_{NN}} = 200$  GeV. The centrality bin is expressed as percentiles of  $\sigma_{AuAu} = 6.9$  b. The last line refers to minimum bias collisions.

Centrality	$\langle T_{AuAu} \rangle$ (mb $^{-1}$ )	$\langle N_{coll} \rangle$	$\langle N_{part} \rangle$	
0-10%	$22.75 \pm 1.56$	$955.4 \pm 93.6$	$325.2 \pm 3.3$	
10-20%	$14.35 \pm 1.00$	$602.6 \pm 59.3$	$234.6 \pm 4.7$	
20-30%	$8.90 \pm 0.72$	$373.8 \pm 39.6$	$166.6 \pm 5.4$	
30-40%	$5.23 \pm 0.44$	$219.8 \pm 22.6$	$114.2 \pm 4.4$	
40-50%	$2.86 \pm 0.28$	$120.3 \pm 13.7$	$74.4 \pm 3.8$	
50-60%	$1.45 \pm 0.23$	$61.0 \pm 9.9$	$45.5 \pm 3.3$	
60-70%	$0.68 \pm 0.18$	$28.5 \pm 7.6$	$25.7 \pm 3.8$	
60-80%	$0.49 \pm 0.14$	$20.4 \pm 5.9$	$19.5 \pm 3.3$	
60-92%	$0.35 \pm 0.10$	$14.5 \pm 4.0$	$14.5 \pm 2.5$	
70-80%	$0.30 \pm 0.10$	$12.4 \pm 4.2$	$13.4 \pm 3.0$	
70-92%	$0.20 \pm 0.06$	$8.3 \pm 2.4$	$9.5 \pm 1.9$	
80-92%	$0.12 \pm 0.03$	$4.9 \pm 1.2$	$6.3 \pm 1.2$	
min. bias	$6.14 \pm 0.45$	$257.8 \pm 25.4$	$109.1 \pm 4.1$	

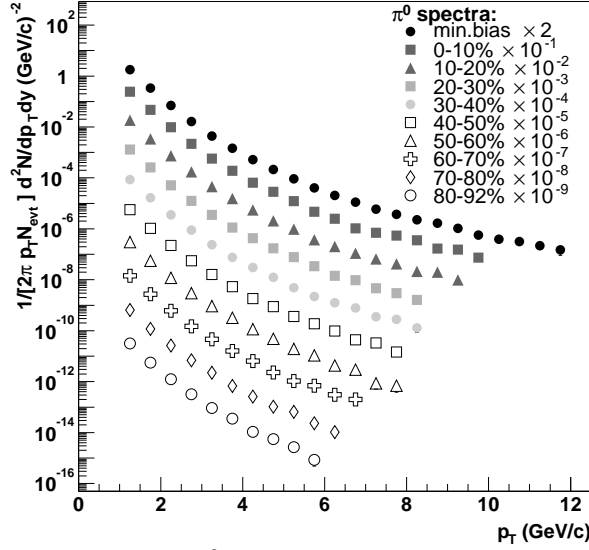


FIG. 1. Invariant  $\pi^0$  yields at mid-rapidity as a function of  $p_T$  for minimum bias and 9 centralities in Au+Au at  $\sqrt{s_{NN}} = 200$  GeV [0-10% (80-92%) is most central (peripheral)].

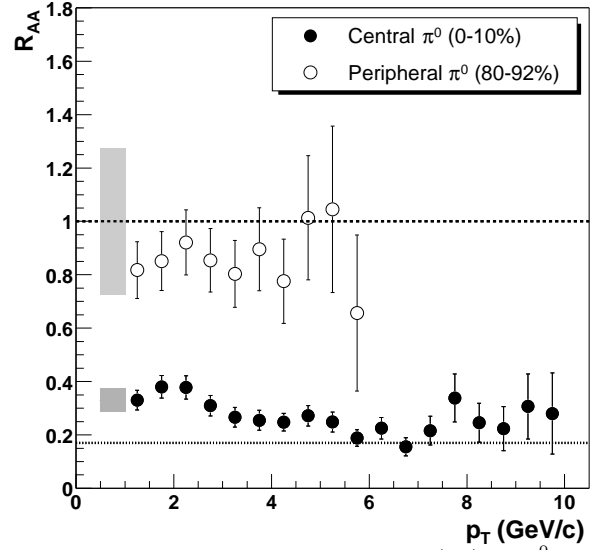


FIG. 2. Nuclear modification factor  $R_{AA}(p_T)$  for  $\pi^0$  in central (closed circles) and peripheral (open circles) Au+Au at  $\sqrt{s_{NN}} = 200$  GeV. The error bars include all point-to-point experimental ( $p + p$ , Au+Au) errors. The shaded bands represent the fractional uncertainties in  $\langle T_{AuAu} \rangle$  and in the  $\pi^0$  yields normalization added in quadrature, which can move all the points up or down together (in the central case the shaded band shown is the fractional error for the first point).

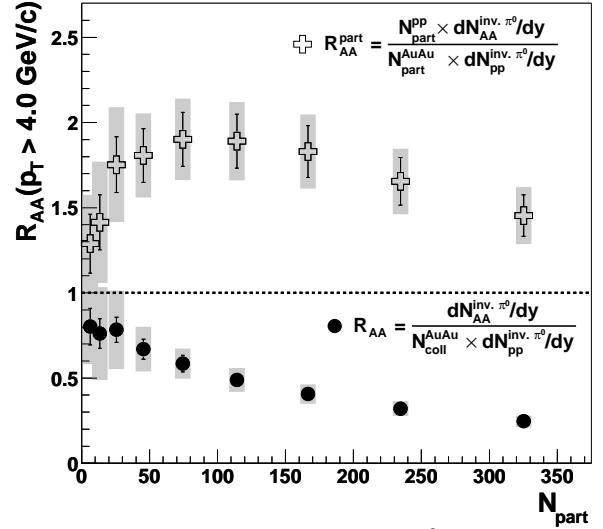


FIG. 3. Ratio of Au+Au over  $p + p$   $\pi^0$  yields integrated above 4 GeV/c and normalized using  $N_{coll}$  (circles) and  $N_{part}$  (crosses), as a function of centrality given by  $N_{part}$ . The errors bands and bars are the same as for Fig. 2.